Understanding the Time Dependent Response of the Martian Upper Atmosphere to Solar Flares and Dust Storms

David J. Pawlowski, Department of Physics and Astronomy, Eastern Michigan University

Contents

1 Objectives

Recently, many studies have been performed which have started to quantify the important processes that govern volatile escape from Mars' atmosphere [*Chassefière and Leblanc*, 2004; *Barabash et al.*, 2007; *Lundin et al.*, 2008]. These studies suggest that several processes are important, including: (1) hot atom (e.g. O, C, N) escape resulting primarily from dissociative recombination of molecular ions, (2) bulk ion outflows created by solar-wind induced electric fields in the ionosphere, (3) pickup ion escape resulting from photo-ionization, electron impact ionization and charge exchange of exospheric neutrals, and (4) sputtering caused by precipitation of pick-up ions and solar energetic particles into the Martian atmosphere, ejecting neutrals to space. The dependence of each of these processes on the state of Mars upper atmosphere suggest that the ionosphere and thermosphere act to regulate the escape of the atmosphere to space. This system is highly dependent on both internal and external forcing. Historically, studies of this region of the Martian atmosphere have been climatological in nature, given characteristic levels of forcing typical of the solar cycle or season. However, in order to further constrain current ,as well as historical levels of escape, a more detailed knowledge of variability of the upper atmospheric system is needed.

Specific Objectives

The overarching goal of the proposed research is to quantify the time-dependent response of the Martian thermosphere and ionosphere to solar flares and dust storms. Specifically, we will:

- Determine how solar flares and dust storms affect the thermospheric and ionospheric densities, temperatures, and winds.
- Increase our understanding of how long perturbations in the ionosphere and thermosphere due to solar flares and dust storms take to dissipate.
- Investigate how the spatial and temporal structure associated with the development and decay of a dust storm affects the upper atmosphere.
- Examine the effect that the dust distribution has on preconditioning the system prior to a solar flare.

Study of the atmospheric escape is not the only reason to better understand the time-dependent behavior of the Martian upper atmosphere. Another reason to improve this understanding is that there is constant interest in sending spacecraft to Mars. Spacecraft that utilize aerobraking or that have orbits that reach thermospheric altitudes, such as the upcoming Maven mission, are subject to, among other space weather effects, atmospheric drag, which can significantly affect the velocity and thus the orbit of the satellite. Providing operational engineers on these missions with a detailed knowledge of the upper atmospheric conditions will make it possible to reduce the possibility of harm coming to the spacecraft. Until recently, lack of observational data has made studying short term or transient phenomenon extremely difficult, if not impossible. However, in the past decade and a half, many useful measurements have been obtained in both the ionosphere and thermosphere that make it possible to study these type of events, and to further quantify the behavior of the system under transient forcing.

Having an understanding of how the system behaves during time-dependent events is, therefore, important to further understanding the escape processes and the overall escape rate of the atmosphere. In addition, there is significant interest in extrapolating these escape processes into the past in order to estimate the evolution of the Mars atmosphere throughout its history. It is thought that earlier in the lifetime of the solar system, the Sun was significantly more active, and therefore it is expected that there would have been many more transient features interacting with Mars, such as solar flares and coronal mass ejections (CMEs). The behavior of Mars' atmosphere during these types of events has yet to be addressed in detail. In particular, several issues related to the behavior of the ionosphere and thermosphere in response to dynamic forcing have yet to be adequately explained. For example:

• What global effects do solar flares and dust storms have on the ionospheric and thermospheric densities, temperatures, and winds?
• How long does the ionosphere and thermosphere remain perturbed following a solar flare?
• How does the spatial and temporal evolution of a dust storm affect the upper atmospheric response?
• How does the distribution of dust effect the response of the system to solar flares?

The goal of this proposed research is to address these questions. In order to do so, we will utilize measurements from a variety of instruments that have sampled the ionosphere and thermosphere throughout the past solar cycle. These data will be used in 2 respects: (1) We will perform an analysis of observational data taken during specific solar flare and dust storm events and, (2) we will use these data to construct inputs to a Mars 3D whole atmosphere global circulation model (GCM) in order to simulate these same events and perform data-model comparisons to help facilitate the interpretation of the observations.

With the availability of accurate thermospheric, ionospheric, dust, and solar EUV/soft X-ray datasets and the recent development and validation of the Mars Global Ionosphere-Thermosphere Model (M-GITM), it is possible to do a systematic investigation into the flow of energy from the Sun into the Martian atmosphere and as it propagates throughout the entire, coupled, system. **The ultimate goal of this proposal is to utilize publicly available data resources in order to significantly increase our understanding of how the upper atmosphere behaves in a time-dependent manner in response to transient forcing. Specifically, we will investigate and quantify the response of the upper atmosphere to solar flares and dust storms.**

2 Observations

In order to investigate the manner in which the Martian upper atmosphere responds to transient forcing, it is necessary to have detailed observations of ionospheric and thermospheric state variables as well as observations of the drivers to the system. For this study, we will make use of measurements of the neutral and electron densities, derived neutral temperature, solar irradiance, and dust opacity, all of which have been observed during the past 1.5 decades via a suite of instruments as discussed below.

2.1 Solar irradiance

Solar extreme ultraviolet (EUV) radiation, including the soft X-ray (XUV) region of the spectrum, corresponding to wavelengths between 0.1 and 200 nm, is absorbed by the Martian neutral gas from roughly 80 km to 200 km. Photons at wavelengths below about 90 nm have enough energy to ionize the background species, while absorption of the longer wavelength photons results primarily in the dissociation of the background gas (CO_2). In either case, the flow of energy through various channels, such as ion production, photoelectron production, electron heating, air glow, etc. [*Torr et al.*, 1980; *Roble*, 1995] results in a percentage (~20% depending on location and solar conditions [*Bougher and Dickinson*, 1988; *Bougher et al.*, 2009; *Fox et al.*, 1996; *Huestis et al.*, 2008]) of the incident energy going into the heating of the neutral gas. The amount of energy that is being absorbed by the thermosphere is important in determining the neutral density both locally and aloft, but it is not the only mechanism that controls the global behavior of the thermosphere. Relatively large ion production rates in this region result in the ionospheric density being significant in comparison to the density of the thermosphere,

therefore, in order to understand the energetics and dynamics of the thermosphere, it is necessary to examine the behavior of the coupled ionosphere and thermosphere system.

Long term measurements of the entire EUV and XUV spectrum have never been available at Mars. Only since 2001 have such measurements been made at Earth. For this reason, several studies have attempted to quantify the activity level of the Sun based on measurements made at a single wavelength. The most common of these proxy based methods, called the $F_{10.7}$ proxy [*Hinteregger et al.*, 1981; *Richards et al.*, 1994; *Tobiska*, 1991; *Woods and Rottman*, 2002], correlates changes in the solar irradiance measured at 10.7 cm to changes in the entire EUV spectrum. While the $F_{10.7}$ has been useful in allowing researchers to study how long term trends in the solar irradiance affect the ionospheres and thermospheres of the planets [e.g. *Fox et al.*, 1996; *Kim et al.*, 1998; *Fox*, 2004], the $F_{10.7}$ does not replicate the short term variability that is observed in parts of the solar XUV and EUV spectrum. For example, Figure 1 shows a plot of the solar XUV flux from 1-8Å as measured by one of the Geostationary Operational Environmental Satellites (GOES) as well as the $F_{10.7}$ during the particularly active month of October, 2003. During certain time periods, the solar flux is extremely variable. The $F_{10.7}$ proxy is limited as it is *only* a proxy of the entire solar EUV spectrum, and therefore isn't ideal for capturing the short term irradiance variations [*Chamberlin et al.*, 2008].

In 2001, with the launch of the Thermosphere-Ionosphere-Mesosphere Energetics and Dynamics (TIMED) mission in orbit around Earth, new, high-resolution measurements of the EUV spectrum became available from the Solar EUV Experiment (SEE) [*Woods et al.*, 2005]. *Chamberlin et al.* [2007] have developed a model of the solar spectrum that makes use of these data along with measurements from GOES, in addition to other proxies, to produce a database of solar spectra at 1 minute intervals and 1 nm resolution between 0.1 and 195 nm. The Flare Irradiance Spectral Model, FISM, allows studies of the upper atmospheric response to solar flares to be performed more accurately than ever before, and is freely available to the community at the FISM website: http://lasp.colorado.edu/lisird/fism/.

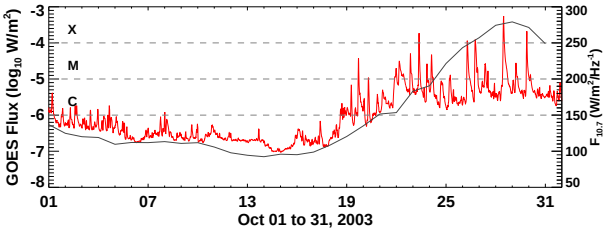

Figure 1: GOES X-ray flux from 1-8Å (red line) and the $F_{10.7}$ (black line) during October, 2003

The availability of data on the EUV and XUV spectrum makes study of the upper atmospheric response to short term solar forcing possible. Not only is this data necessary for investigating the Martian upper atmospheric response to solar flares, but it is also useful for studying the behavior of the thermosphere under other forcing, such as dust storms, since the upper atmosphere may respond differently to a dust storm event during quiet solar conditions than it does during active ones.

2.2 Observations of Transient Events

Recently, ionospheric observations from 1998-2005 have been made by the MGS Radio Science experiment [*Hinson et al.*, 1999], providing an extensive set of measurements of the electron density. Thousands of high latitude electron density profiles in the solar zenith angle range 71-89 degrees have been returned. All of these profiles are available on the PDS and a publicly available Stanford University website, http://nova.stanford.edu/projects/mgs/eds-public.html.

In addition to ionospheric measurements, observations of the thermosphere have been made during MGS and Odyssey aerobraking campaigns. In particular, the MGS z-axis accelerometer has provided measurements of the thermospheric density and derived temperature and pressure during the 2 aerobraking phases of the mission (1997-1999),

resulting in over 1200 vertical profiles of the thermospheric structure [*Keating et al.*, 1998]. Analysis of these measurements has indicated that there is significant variability in the Martian thermosphere due to a number of sources [*Keating et al.*, 1998; *Bougher et al.*, 1999; *Withers et al.*, 2003; *Bougher et al.*, 2004; *Angelats i Coll et al.*, 2004; *Moudden and Forbes*, 2008, 2010, e.g.]. *Keating et al.* [1998] show that the upper atmospheric density could vary by more than a factor of 2 (especially during a regional dust storm), even when accounting for altitude, latitude, local time and seasonal variations. Both MGS and Odyssey aerobraking datasets from their respective acclerometers are available on the PDS.

Finally, lower atmosphere dust opacities were measured by the MGS Thermal Emission Spectrometer (TES) and the Odyssey THEMIS instruments [*Smith*, 2004, 2009, e.g.], together spanning Martian seasons over more than a decade (from 1998 to the present). From these measurements, it is well documented that the dust opacity within the Mars atmosphere undergoes strong seasonal variability as well as inter-annual variations. In particular, the dust loads during the perihelion season (Ls˜240-270 degrees) display wide interannual variability in terms of (1) the time evolution of the dust opacity, (2) the number, strength, and latitudinal extent of dust storm events, and (3) the dust storm timing and duration [*McDunn et al.*, 2010, e.g.]. Due to this large variability of the spatial (vertical and horizontal) distribution of dust in the Martian lower atmosphere, significant impacts aloft are expected in the thermosphere. These MGS/TES and Odyssey/THEMIS dust opacity datasets are publicly available on the PDS.

2.2.1 Dust Storm Responses

Several studies suggest that one of the sources of thermospheric variability that is particularly difficult to predict are lower atmospheric dust storms. For example, *Bougher et al.* [2001, 2004]; *Wang and Nielsen* [2003] show that during such an event the altitude of the ionospheric peak can be highly variable as a result of inflation of the atmosphere as a whole. Also, *Bougher et al.* [1999] examine the Noachis event, which lasted from November 25, 1997 through January 12, 1998 [*Keating et al.*, 1998]. During this event, MGS was able to observe the behavior of the lower atmospheric temperatures (using the TES instrument), dust opacities (TES), and upper atmospheric densities (accelerometer) simultaneously. *Bougher et al.* [1999] performed a data-model comparison of this event using the coupled Mars Global Circulation Model (MGCM) (0-80 km) and the Mars Thermosphere General Circulation Model (MTGCM) (70-250 km). Figure 2 shows the results of this comparison for the thermospheric density near the spacecraft periapsis (130 km).

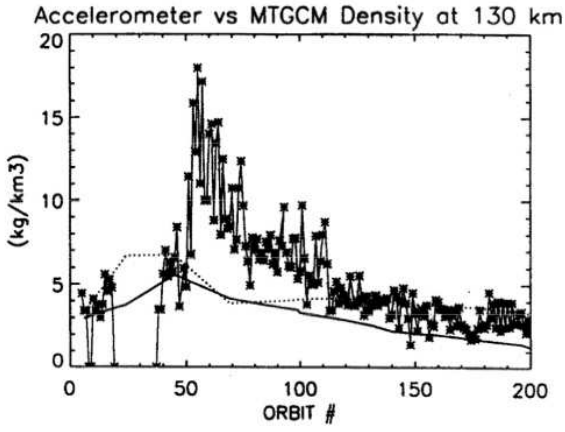

Figure 2: MGS accelerometer densities near periapsis (asterisks) as well as coupled MGCM-MTGCM results using tau = 0.3 (solid line) and tau = 1.0 (dotted line) [*Bougher et al.*, 1999].

The coupled model was run three times for this study, once utilizing a moderate (tau = 0.1) globally uniform visible dust opacity, and again using an elevated (tau = 1.0) opacity, and a third time using a more realistic dust distribution (results in Figure 3). While the model is able to reproduce pre- and post-storm average densities reasonably well, when the model is run using a uniform horizontal dust distribution, even for the

Interval	Profiles	Ls Coverage	Latitude (deg)
MGS1: 16-Sep-97 to 27-Mar-98	200	180-300	35N-65N
MGS2: 24-Sep-98 to 4-Feb-99	600	34-92	50N-80S and 80S-30S
MO: 28-OCT-01 to 11-Jan-02	300	260-310	70N-80N to 80N-15N
MRO: 30-Mar-06 to 30-Aug-06	450	35-99	80S-85S to 80S-12N

Table 1: Aerobraking sampling parameters for 4 campaigns at 130km for imbound legs of spacecraft aeropasses.

dusty case, the results do not show nearly the same variability in density as do the observations. Even when a more realistic distribution is used, the model only shows an density increase of 70% compared to 200% in the data.

These results demonstrate that there is a lack of understanding of the interaction between the lower and upper atmospheres during these types of events. Several questions regarding the upper atmospheric response to dust storms remain to be answered:
• What processes dominants during a storm event that lead to such observed changes in the thermospheric density?
• How does the horizontal distribution of the dust affect the response?
• How does the response depend on the background state of the atmosphere?

2.2.2 Solar Flare Responses

While high accuracy measurements of the thermospheric density at Mars are available, thanks primarily to the MGS, Mars Odyssey (MO), and Mars Reconnaissance Orbiter (MRO), most of these measurements were taken during the aerobraking phases of the missions, and so measurements are available only for limited time periods (Table 1).

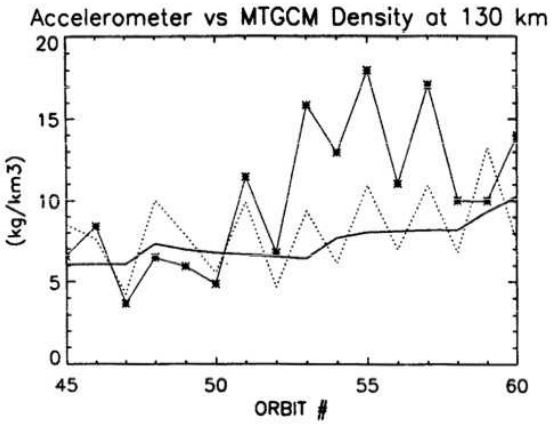

Figure 3: MGS accelerometer densities near periapsis (asterisks) as well as coupled MGCM-MTGCM results using a spatially and temporally dependent dust optical depth including longitude variations (dotted line) and not including longitude variations (solid line) [*Bougher et al.*, 1999].

In order to be able to quantify the thermospheric response to a solar flare, it is necessary to have some specification of the time dependent solar irradiance, and since the best measurements are taken at Earth, we can only use this data for flares that occurred when the Earth–Sun–Mars angle is within a certain range (at least 90°). Ideally, only flares that occurred after late 2001, when TIMED/SEE measurements became available would be studied, as there is a relevant FISM data product. The combination of these constraints, in addition to the relatively small windows when density data was obtained, makes performing a detailed analysis of the thermospheric response to solar flares limited if only neutral data is used. For this reason, it is necessary to additionally turn to ionospheric measurements to obtain a more detailed picture. The availability of long-term measurements of the ionospheric density from MGS radio occultations in particular make this possible. Previous studies have already begun to use these data to quantify the effects of solar activity [*Mendillo et al.*, 2003; *Martinis et al.*, 2003; *Fox and Yeager*, 2009, e.g.] and solar flares [*Mendillo et al.*, 2006; *Mahajan et al.*, 2009] on the ionosphere. *Withers* [2009] provides a review of the state of knowledge of variability in the ionosphere, which includes discussion of the ionospheric effects of solar flares. *Mendillo*

et al. [2006] shows that the largest ionospheric perturbations occur below the Mars F_1 ionospheric layer, and that the electron density in the E layer can increase by a factor of 2 or more. An example of these observations is shown in Figure 4 [*Withers et al.*, 2005], which plots several electron density profiles taken in succession. The red profile was obtained during a solar flare that occurred on May 31, 2003 just before 3:00 UT.

In one of the most interesting studies, *Withers et al.* [2006] use MGS occultation observations to show that at times the E layer electron density can be unusually small, possibly due to low ion production rates or high ion loss rates. An example of one of these events is shown in Figure 5. While the cause of these features has not been addressed, it is possible that coupling with the neutral atmosphere may be responsible [*Withers*, 2009] and the variable EUV conditions may ultimately be the culprit. *Pawlowski and Ridley* [2009a] show that at Earth, the ionosphere can be depleted during a solar flare as a result of perturbations in the thermosphere.

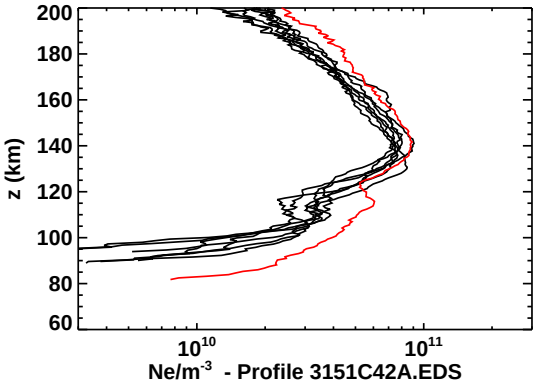

Figure 4: MGS radio occultation data surrounding the May 31, 2003 solar flare.

3 Expected Scientific Significance

We will approach addressing the goal of quantifying the upper atmospheric response to solar flares and dust storms by focusing on investigating the nonlinear coupling between the Sun and the ionosphere and thermosphere, and determine the system level response to highly variable energy input from the Sun while accounting for the dynamic behavior of the lower atmosphere. In using this approach, we will go beyond the practice of performing case studies, and make use of observations of several state variables and drivers in order to follow the energy as it is transferred throughout the system. Also, we will use a global model of the atmosphere to help interpret the data and fill in gaps, so that we can better understand the timescales involved with the system absorbing, transferring, and removing extra solar energy and how the flow of energy in the lower atmosphere propagates upwards and affects the ionosphere and thermosphere. Specifically, we will address the following questions:

3.1 What global effects do solar flares and dust storms have on the thermospheric and ionospheric density, temperature and winds?

The studies that are discussed in Section 2.2 have been incredibly valuable for showing the Mars atmosphere responds to transient forcing. Still, they only focus a limited number of individual events, and have not been able to assemble a complete picture of the flow of energy from the Sun, into the atmosphere, to the surface and back out again. There is need for a more detailed understanding of the behavior of the upper

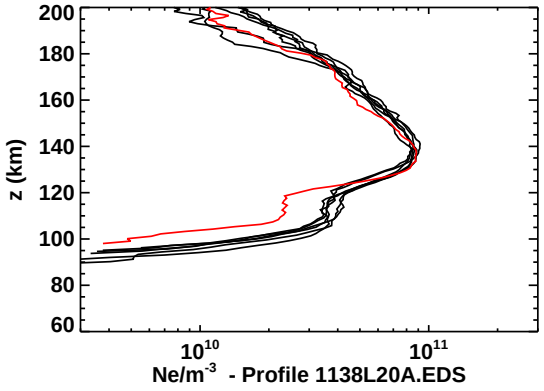

Figure 5: MGS radio occultation data on May 18, 2001.

atmosphere under this type of transient forcing in order to better understand outstanding science questions like atmospheric escape, and to be better prepared for the adverse affects of space weather for future missions, such as Maven.

Given the availability of electron and neutral density information in combination with measurements of the solar EUV and XUV spectrum, analysis of the behavior of the ionosphere and thermosphere during transient events is possible. In order to quantify the effect that flares and dust storms have on the atmosphere, we will utilize the existing observations of the ionosphere and thermosphere variables in combination with M-GITM. We will use observations of the system drivers to tell us how much extra energy is in the system, and analysis of the upper atmospheric measurements will help constrain the possible perturbations that the system experiences. Also, we will perform simulations of each of these events in order to gain a detailed understanding of the flow of energy as it is absorbed by the atmosphere, travels throughout the ionosphere-thermosphere system, and is eventually dissipated during and after an event. By comparing observations to the simulation results, we will develop an understanding of the dynamical and compositional changes in the thermosphere that affect the ionosphere and vica versa. Specifically, we will attempt to accomplish this goal by:

- Studying the coupled response to solar flares and dust storms by utilizing the best measurements possible of the solar EUV/XUV spectrum and analyzing data from the neutral and ion instruments onboard MGS and Odyssey.
  - For solar flares, we will characterize the thermospheric and ionospheric response based on several characteristics, such as: (1) the flare magnitude, (2) the total incident energy above background, and (3) the background state of the atmosphere.
  - We will investigate if and how disturbances in the thermosphere affect the ionosphere, and attempt to understand the cause of the negative flare effects discussed by [*Withers*, 2009].
  - For dust storms, we will characterize the response based on similar characteristics: (1) The maximum dust opacity, (2) the background state of the thermosphere, and (3) the horizontal scale of the dust distribution.
- Conducting simulations of specific time periods during which solar flares and dust storms have occurred and affected the Martian upper atmosphere to aid in the interpretation of the observations and provide a detailed picture of the flow of energy as it passes through various channels throughout the entire atmosphere.
- Utilizing the model to constrain the effect of the uncertainty in solar irradiance measurements by simulating each event repeatedly using a range of solar fluxes to determine a range of responses that one may expect in the thermosphere and ionosphere system.

We will begin by expanding the number of case studies that have been performed. Table 2 shows information about 7 flare events that will be studied. These were chosen based on several factors: (1) Availability of observations of ionospheric and thermospheric data; (2) availability of observations of EUV/XUV fluxes; (3) Mars–Sun–Earth angle less than 90°; (4) flare magnitude. With the exception of the November 1998 event, high temporal resolution FISM data is available for each of these simulations. Prior to study, the EUV/XUV data will to be scaled to account for the Earth–Mars distance and the Mars–Sun–Earth angle. If FISM data is not available, we will utilize measurements from the GOES satellites, the $F_{10.7}$and other solar proxies, such as Lyman-α to provide insight into the behavior of the soft X-rays.

The dust storm events to be studied are shown in Table 3. Again, these events were chosen based on available measurements of the state variables, as well as the dust opacity.

Event Date	Magnitude	Datasets Available
11-28-98	X3	MGS ACC, GOES
11-26-00	X4	MGS RS, FISM
04-02-01	X16	MGS RS, FISM
04-15-01	X11	MGS RS, FISM
12-13-01	X6	MO ACC, FISM(SEE)
12-28-01	X6	MO ACC, FISM(SEE)
05-28-03	X3	MGS RS, FISM(SEE)

Table 2: List of solar flare events for proposed study. SEE data was only available for incorporation into FISM after 2001.

3.2 How long does the ionosphere and thermosphere remain perturbed following a solar flare?

Unlike dust storms, which tend to last weeks to months, solar flares last from minutes to hours. This means that the resulting ionospheric and thermospheric perturbation will commence and end on a relatively short time scale. Typically, it was thought that flare effects in the upper atmosphere are directly driven and last as long as the flare. *Pawlowski and Ridley* [2008] show that at Earth, this is not necessarily the case, and rather the flare creates a disturbance that propagates from the dayside towards the nightside, taking a few hours. Figure 6 shows the results for a simulation of the thermospheric density at Mars in response to the October 28, 2003 X17 solar flare that lead to the so called Halloween Storm that affected Earth. The flare began at about 11:00 UT and ended around 18:00 UT. FISM data was used accounting only for the Earth–Mars distance.

Storm	Ls (onset)	Date (onset)	Data
Noachis (Reg.)	224	25-Nov-97	TES, ACC, RS
2001 (Global)	185	25-Jun-01	RS
2007 (Global)	265	03-Jul-07	THEMIS

Table 3: List of dust storm events for proposed study.

The model indicates that the thermosphere has not recovered by the time the flare has ended (˜18:00 UT on the 28^{th}). In this case, the thermosphere remains perturbed for many hours after the event, and never fully returns to a background level due to a slightly elevated solar flux post-flare. On the 29^{th}, another flare occurs and the density is again perturbed. Like Earth, the Mars atmosphere responds to the solar flare by launching a traveling atmospheric disturbance towards the nightside. Convergence on the nightside creates the secondary maximum that is seen around 20 UT on the 28^{th} in the results.

Observations and simulations at Earth [*Sutton et al.*, 2003; *Pawlowski and Ridley*, 2008] show that the perturbations in the thermosphere can last up to 12 hours following a flare. In order for the atmosphere to return to its nominal state, the additional energy that was absorbed during the flare must be lost again. This is primarily accomplished via radiative cooling, though molecular conduction plays a role as well. At Mars, these processes play an important role in the global energy budget [*Bougher et al.*, 1999, 2000, 2009], however, their relative importance is different, as are the primary radiative cooling mechanisms. At Earth, NO cooling is the primary radiative cooling agent, with O playing a lesser role and CO_2 being important in the lowest layers of the thermosphere. At Mars, it is CO_2 cooling that is by far the most important. This difference should make the behavior of the upper atmosphere at Mars different than the behavior at Earth. This is indeed the case here. As shown in [*Pawlowski and Ridley*, 2008], using the terrestrial version of GITM, this same event was simulated at Earth. The maximum dayside perturbation at Earth was significantly smaller that that at Mars. This behavior is unexpected, given that the relative distance between Earth and Mars was accounted

for in the solar flux data. **It is clear that the cooling mechanisms must be operating on different time scales, and exactly how these mechanisms respond to the influx of EUV radiation is one of the main issues the we intend to address as part of this study.**

Figure 6 also shows that the ionosphere is significantly perturbed during a flare, especially on local scales. While the ionospheric perturbations seem to mirror the behavior of the solar flux more than the thermospheric results, the ionosphere is still disturbed after the flare has ended. The model suggests that there may be a two-stage recovery in the ionospheric density, possibly as a result of changes in the thermospheric concentrations affecting the loss rates. In quantifying the amount of time the atmosphere remains perturbed following a solar flare, we will utilize the observations of the electron and neutral density in combination with results from the flare event simulations outlined above. **We will focus on understanding how the cooling mechanisms respond to the additional energy, and also investigate the manner in which increased electron densities balance with changes in the neutral concentrations to determine the decay rate for the ionosphere**.

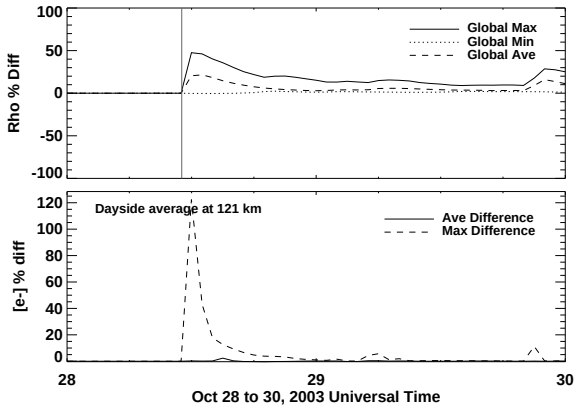

Figure 6: (Top) Thermospheric density percent difference results at 200 km from a M-GITM simulation of the October 28, 2003 solar flare event. The global maximum (solid line), average (dashed line) and minimum (dotted line) are shown. The electron density dayside average (solid line) and dayside maximum (dashed line) percent difference at 121 km is also shown (bottom).

3.3 How does the spatial and temporal structure associated with the development and decay of a dust storm affect the upper atmosphere?

The response of the thermosphere and ionosphere to dust storms has not been studied as in-depth as other aspects of the upper atmosphere, such as the response of the system to tidal forcing [*Angelats i Coll et al.*, 2004; *Bougher et al.*, 2004; *González-Galindo et al.*, 2009; *Moudden and Forbes*, 2008, 2010]. While preliminary studies have investigated the perturbations observed in the ionosphere and thermosphere during a dust storm *Bougher et al.* [1999]; *Wang and Nielsen* [2003] and show that the Martian atmosphere can be significantly disturbed during a regional dust storm, little work has been done to determine how the spatial and temporal structure of both regional and global storms affect the combined response of the thermosphere and ionosphere. With the availability of measurements of ion and neutral densities, in addition to observations of the lower atmospheric dust distribution, it is possible to further quantify the influence that dust plays on the state of the ionosphere and thermosphere. Indeed, observations of the dust opacity show that the dust distribution can be highly variable both in space and in time. For example, Figure 7, which shows the dust opacity as observed by TES in 2001 at Ls = 182 – 207 in 5°increments, corresponding to June 21 - August 2, 2001, indicates that there can be considerable spatial structure during a dust storm and that events that start off on small, local scales can quickly evolve to become more global.

Given the highly non-linear nature of the coupling between the lower and upper atmosphere, it is expected that changes in the dust distribution on relatively small spatial or temporal time scales will have more significant effects aloft. We will investigate dust storms that have occurred since 1997, focusing on those listed in Table 3. During these

events, measurements of the dust opacity were made by the TES instrument and/or Themis.

Based on observations of these events, we will attempt to better understand the non-linear behavior of the coupled lower and upper atmosphere by:

- Using simultaneous measurements of the MGS/TES or Odyssey/THEMIS dust opacities and the atmospheric state variables to study dust events that have taken place throughout the last solar cycle.
- Using TES or THEMIS dust opacity observations to construct time and spatially dependent inputs to drive M-GITM. The results will focus on developing an understanding of how energy and momentum is transferred from the lower atmosphere during a dust storm, to the upper atmosphere.
- Performing several idealized M-GITM simulations that use dust opacities that are based on TES/THEMIS observations, but account for uncertainty in the observations in order to constrain the possible upper atmospheric perturbation outcomes.

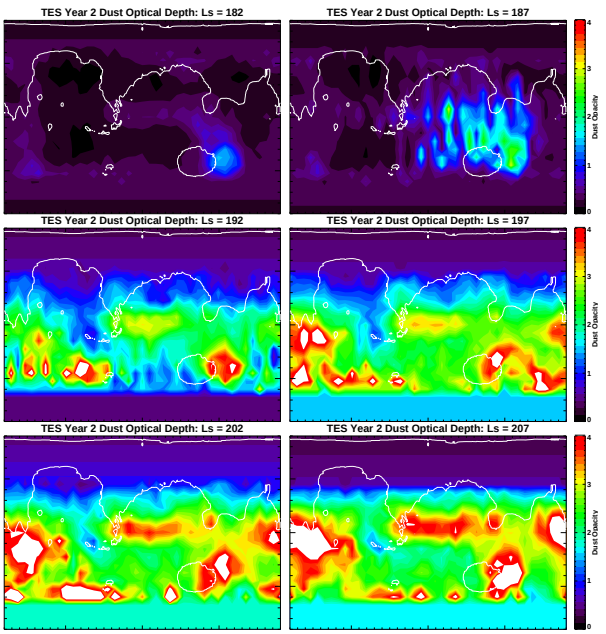

Figure 7: 6 contour plots of the visible dust opacity taken during the beginning of the 2001 global dust storm. Each snapshot is separated by 5°in L_s.

3.4 What effect does the dust distribution have on preconditioning the upper atmospheric system?

Ultimately, the behavior of the atmosphere during a solar flare and dust storm are similar. In both cases, the atmosphere responds by expanding and contracting, or breathing. During a dust storm, the lower atmosphere undergoes added aerosol heating causing an expansion. This is felt aloft, where the pressure at a given altitude is increased. A consequence of this is that the thermosphere is essentially inflated, and the absorption of solar radiation will take place at a higher altitude. It is expected that the ionospheric structure would then be altered as well, given that the altitude at which the ionizing radiation reaches an optical depth of unity would be increased. The question then, is how does the atmosphere deal with this two fold atmospheric expansion? A study at Earth [*Pawlowski and Ridley*, 2011] showed that when the atmosphere is in an enhanced state vs. a nominal state, the perturbation that results from a solar flare will be larger (by percentage) for the nominal case. However, in terms of absolute difference, the atmosphere is perturbed by a greater amount when the atmosphere is in an excited state. This has important consequences for aerobraking maneuvers and for orbiters that reach thermospheric altitudes, such as Maven.

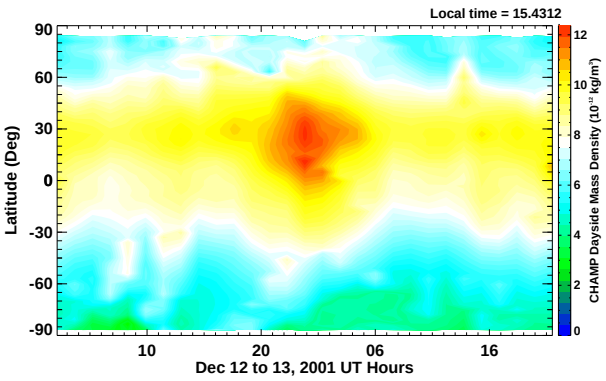

Figure 8: The terrestrial thermospheric density at 400 km as measured by the CHAMP satellite on December 12 - 13, 2001 during several repetitive solar flare events.

Figure 8 illustrates the effect of preconditioning in the terrestrial thermosphere, and shows observations of the density at 400km from the CHAMP satellite during a series of solar flares in December of 2001. On December 12, beginning at around 19 UT, 3 consecutive M-class flares occurred within the span of 6 hours, ending just before 0 UT on the 13^{th}. These events cause the maximum that occurs in the dayside density. At around 14 UT on the 13^{th} there was a single, X-class flare. The perturbation that resulted from the 3 consecutive flares dwarfs any perturbation following the larger flare.

It is expected that the response to flares at Mars during a dust storm event is similar to this terrestrial case; if the flare occurs when the atmosphere is already perturbed due to a dust storm, the perturbation will be significantly larger than if the atmosphere were not perturbed. As part of this study, we plan to investigate the effects of this type of preconditioning on the atmosphere. Ionospheric observations made during different dust conditions (Table 2 will provide insight into the behavior of the system, but we will further constrain the possible perturbations using M-GITM to perform idealized simulations of the ionosphere and thermosphere system based on observations of dust opacities during both localized and global dust storms. We will perform several sets of simulations for a flare event where each set of simulations uses the observed opacities as constraints on the lower atmospheric forcing. For example, for one set, we will run the model with varying levels of globally integrated uniform dust opacities (i.e. tau = 0.5, 0.7, 1.0, 2.0, etc.) that is held constant throughout the duration of a flare event and compare that with a simulation in which the globally integrated dust opacity is a more nominal 0.3. In another set, we will use similar opacities, however, we will require that the opacities be restricted to one hemisphere, in another set, a particular geographical location.

The results from our investigation into the manner in which the upper atmosphere responds to the spatial and temporal evolution of a dust storm should help shed light on possible "worst case scenarios" for the occurrence of a solar flare, and we can utilize these insights to perform additional simulations to further constrain the range of possible atmospheric perturbations that are expected for a range of dust conditions. We will run many flare events in the manner outlined above, and focus on addressing the following issues:

• For a given flare integrated energy input, what is the worst possible time that a flare can occur in terms of a possible lower atmospheric dust distribution?

• How linear is the dependence of the response to the solar flare on the strength of the dust storm (i.e. the opacity)?

• Is there a difference between the decay time of the atmosphere following a flare for different dust conditions?

4 The Mars Global Ionosphere–Thermosphere Model

4.1 Model Formulation, Development and Inputs

While the proposed work focuses on using data to investigate the time-dependent response to transient forcing, the use of M–GITM is necessary to fully understand the transfer of energy and momentum from the Sun and throughout the atmosphere. M-GITM is currently undergoing final stages of validation at the U. of Michigan. This effort essentially combines the terrestrial GITM framework (for a complete description of the numerics in GITM, see *Ridley et al.* [2006]) with Mars fundamental physical parameters, ion-neutral chemistry, and key radiative processes in order to capture the basic observed features of the thermal, compositional, and dynamical structure of the Mars atmosphere from the ground to ˜300 km. This comprehensive 6-year model development, testing and validation effort has been ongoing since 2006, and is now in its final year of NSF support.

GITM is a 3-D spherical code that was initially developed to simulate the terrestrial thermosphere - ionosphere system using an altitude based vertical coordinate [*Ridley et al.*, 2006; *Deng et al.*, 2008, e.g.] and has been used to address a range of space weather related issues [*Ridley et al.*, 2006; *Deng and Ridley*, 2007; *Deng et al.*, 2008; *Pawlowski et al.*, 2008; *Pawlowski and Ridley*, 2009a; *Pawlowski and Ridley*, 2011]. The altitude based system allows for the relaxation of the hydrostatic equilibrium assumption and enables the model to resolve sound and gravity waves in both the vertical and horizontal directions. GITM solves for the bulk horizontal neutral winds, while in the vertical direction, the momentum equation is solved for each of the major species and the bulk vertical winds are specified as a mass density weighted average of the individual vertical velocities. The model is fully parallel and utilizes a block-based 2-D (latitude and longitude) domain decomposition that allows the model to have a flexible horizontal resolution that can be specified at run-time.

Unlike at Earth, M-GITM simulates the conditions of the Martian atmosphere all the way to the surface. The formulations and subroutines required for incorporation into the new M-GITM code have largely been taken from existing Mars GCM codes. For the Mars lower atmosphere (0-80 km), a state-of-the-art correlated-k radiation code was adapted from the NASA Ames MGCM [*Haberle et al.*, 2003] for incorporation into M-GITM. This provides solar heating (long and short wavelength), seasonal aerosol heating, and CO2 15-micron cooling in the LTE region of the Mars atmosphere (below 80 km). Typically, dust opacity distributions are prescribed based upon: (a) assumed globally uniform dust opacities, or (b) empirical dust opacity maps obtained from MGS/TES, and Odyssey/THEMIS measurements [*Smith*, 2004, 2009; *McDunn et al.*, 2010]. Finally, a simple formulation for Mars surface temperatures, required for the radiative transfer code, is used based upon Mars empirical temperatures.

For the Mars upper atmosphere (˜80 to 300 km), a fast formulation for NLTE CO2 15-micron cooling has been implemented [*López-Valverde et al.*, 1998; *Bougher et al.*, 2006], along with a correction for NLTE near-IR heating rates (˜80-120 km) using an extension of the correlated-k radiation code. The EUV-UV heating routines have been modified for a CO2 atmosphere by incorporating an expanded set of cross sections and yields. These additions specify the in-situ heating (EUV-UV), dissociation, and ionization rates spanning ˜80 to 300 km. Finally, a comprehensive set of ˜30 key ion-neutral chemistry reactions and rates has been incorporated into the code [*Fox and Sung*, 2001], based upon those used in the MTGCM [*Bougher et al.*, 2004, e.g.]. A sub-cycling technique is used to handle the chemistry, so that several chemical time steps may be used for each advective time step. Like the neutrals, M-GITM is capable of allowing different ion species to have different vertical velocities, though typically a bulk vertical ion velocity is calculated assuming contributions from neutral drag, the ion pressure gradient, gravity, and the polarization electric field are the dominant forcing terms.

For the entire atmosphere, the M-GITM dynamical core solver was modified to utilize a terrain following coordinate system, and the Martian topography is now incorporated into the M-GITM code making use of MGS Mars Orbiter Laser Altimeter (MOLA) topographic data files [*Smith and Zuber*, 1996]. In addition, a simplified gravity wave momentum deposition scheme was recently added, and is being tested through comparisons with the AMES GCM and MTCGM.

The M-GITM code presently simulates the following neutral and plasma fields globally: Neutral temperatures are solved for self-consistently, but ion and electron temperatures are presently prescribed based upon Viking measurements. Key neutral species (10) include: CO2, CO, O, N2, O2, N(4S), N(2D), NO, Ar and He. Key ion species (5) include: O+, O2+, CO2+, N2+ and NO+. Currently, horizontal ion velocities are not calculated. Typically, M–GITM simulations are conducted for a 2.5° latitude x5 ° lon-

gitude regular horizontal grid, with a constant 2.5 km vertical resolution (˜0.25 scale height) above the lowest ˜80 km. A stretched vertical grid is used at lower altitudes to accommodate the variable terrain.

4.2 M-GITM Validation

Detailed M-GITM simulations have been conducted over the past year, spanning various seasonal, solar cycle, and dust conditions. Model validation thus far has focused upon simulations for Ls = 0, 90, and 270 for both solar minimum (F10.7 = 70) and solar maximum (F10.7 = 200) conditions. Specific studies compare M-GITM simulated temperatures and neutral/ion densities against: (a) in-situ Viking 1 descent measurements for solar minimum/aphelion conditions, and (b) very limited Mariner 6-7 flyby measurements for solar maximum/perihelion conditions. Figure 9 illustrates sample results from these extreme cases.

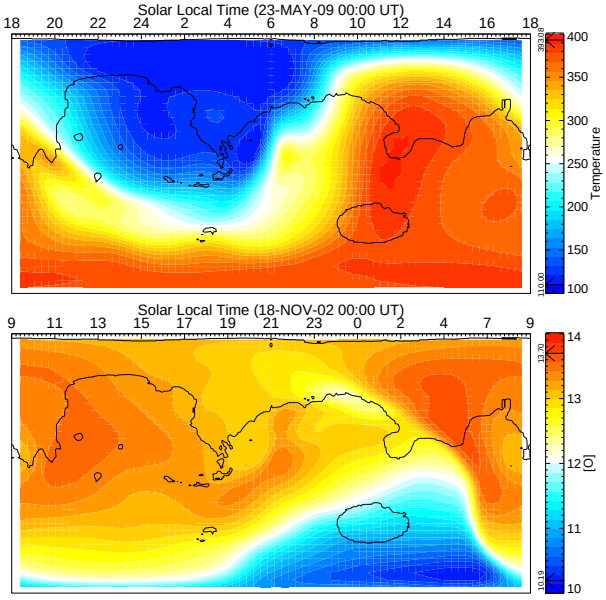

Figure 9: M-GITM results for (top) exospheric temperatures during Mariner conditions and (bottom) O density during Viking Conditions.

Recent studies by [*Pawlowski et al.*, 2010; *Bougher and Huestis*, 2010; *Bougher et al.*, 2011c,b,a; *Pawlowski et al.*, 2011] indicate the model is capturing observed global features: (1) Simulated mean dayside exospheric temperatures are close to data estimated values (185 to 350 K) [*Bougher et al.*, 2009; *Bougher and Huestis*, 2010]. (2) Divergence of winds from the mid-afternoon near the sub-solar latitude, and convergence on the nightside in the mid-to-high latitudes of the winter hemisphere (maximum wind magnitudes approach 200-300 m/s). (3) Nightside mesopause temperatures (90-100 K) are similar to those observed for this season [*McDunn et al.*, 2010]. (4) Aphelion/solar minimum photochemical ionosphere provides realistic dayside ion densities below ˜200 km, in agreement with Viking observations [*Hanson et al.*, 1977]. (5) Winter polar warming at low thermospheric altitudes is minimal for Viking conditions, in agreement with limited MGS aerobraking observations [*Bougher et al.*, 2006]. These sample M-GITM simulated outputs illustrate that model validation studies are proceeding well.

5 Technical Approach and Methodology

The overall goal of this proposed effort is to quantify the manner in which the Martian ionosphere-thermosphere system responds to changing solar EUV-XUV conditions and dynamic lower atmospheric forcing during dust storms, and how the non-linearities within the system affect that response. This is quite difficult to do using observations alone, therefore, in combination with analysis of measurements, we will simulate several realistic events for which observations are available of the state variables of the system, as well as the driving conditions. In order to investigate the physics of the non-linear system, we will use several methodologies. For example, we will: (1) Statistically analyze the data to determine what conditions exist in both the EUV spectra and the dust distributions that lead to upper atmospheric disturbances vs. those that don't. (2) Utilize measurements of the ionosphere in combination with results from the model to help

infer information about changes in the thermosphere. (3) Simulate all events with a distribution of inputs (i.e., slightly smaller/larger flare, slightly less/more dusty atmosphere, nominal background conditions/enhanced background, etc.) to determine the distribution of responses. (4) Utilize idealized conditions constrained by observations to drive simulations in order to quantify the possible range of perturbations.

6 NASA Relevance and Perceived Impact

This proposal is addressed to the NASA Mars Data Analysis Program (MDAP) since the research is focused upon the use of observations from the MGS and Mars Odyssey missions. This project will enhance the scientific return from these missions and provide information on the Mars atmosphere that will benefit future missions, such as MAVEN (2013-2015). Also, the MDAP program document specifically refers to a need for "improved atmospheric models that further the understanding and forecasting of Mars atmospheric conditions that affect the orbital trajectories of spacecraft, and/or the safe passage of spacecraft through the atmosphere, including aerobraking and aerocapture."

The proposed research is also relevant to the following Mars Exploration Program [*MEPAG Goals Committee*, 2010] objectives:

Characterize Mars' Atmosphere, Present Climate, and Climate Processes Under Current Orbital Configuration

• The primary focus of this proposal is to further develop understanding of the time dependent response of the coupled Mars ionosphere-thermosphere system to dynamic forcing. Having knowledge of how the ionosphere and thermosphere responds to these types of events in an integral part to fully characterizing the Mars atmosphere.

Quantify the processes that link the Mars lower and upper atmospheres

• We will investigate the effects that dust storms have on the ionosphere and thermosphere system using a **ground to exobase approach**.

Determine the rates of escape of key species from the Martian atmosphere, their correlation with seasonal and **solar variability**, and their connection with lower atmosphere phenomenon (e.g., **dust storms**)

• This proposal specifically addresses the response of the upper atmosphere to solar variability and dust storms. We have a detailed plan to quantify this response in several ways through the use of publicly available data and the utilization of a global ground–to–exobase model.

7 Management Plan and Work Schedule

David Pawlowski, PI is an Assistant Professor in the Physics and Astronomy department at Eastern Michigan University and will be responsible for the overall success of the project. Dr. Pawlowski has been involved in the development, testing, and use of the GITM code [*Ridley et al.*, 2006; *Pawlowski and Ridley*, 2009b] at Earth and Mars for the past 6 years and, using GITM, has addressed the terrestrial thermospheric and ionospheric response to solar flares [*Pawlowski and Ridley*, 2008; *Pawlowski and Ridley*, 2009a; *Pawlowski and Ridley*, 2011] and other external forcing [*Pawlowski et al.*, 2008].

Stephen Bougher, Co-I, a Collegiate Research Professor at the University of Michigan's Atmospheric, Oceanic, and Space Science department, has served on the aerobraking teams for MGS (1997–1999), Odyssey (2001–2002), and MRO (2006), and is an expert on spacecraft data sets and model simulations that address Mars mesosphere–thermosphere–ionosphere structure and dynamics [*Bougher and Dickinson*, 1988; *Bougher et al.*, 1999; *Bougher et al.*, 2004, 2006, 2009, e.g]. Dr. Bougher will assist in interpretation of the measurements from the various instruments aboard MGS and Odyssey spacecraft. He will specifically conduct M-GITM dust storm simulations, as well as aiding in the analysis of the results from both solar flare and dust storm M-GITM simulations.

Finally,Bougher will mentor a UM graduate student who will be involved in conducting M-GITM simulations as well.

Phi Chamberlin, Collaborator is the creator of the Flare Irradiance Spectral Model (FISM) [*Chamberlin et al.*, 2008] and is an expert in the interpretation of measurements of the solar EUV spectrum. Dr. Chamberlin will assist in interpreting the behavior of the EUV/XUV radiation, and help adapt FISM data for use at Mars.

Jim Murphy, Collaborator is an expert on spacecraft data sets and model simulations that address the Martian lower atmosphere, and has been investigating the temporal and spatial behavior of dust storms on Mars for the last several decades [*Murphy et al.*, 1990, 1995; *Bridger and Murphy*, 1998, e.g.]. Dr. Murphy will assist in the interpretation of dust opacity measurements as well has help produce 2-D maps of the opacity during dust storms for input into M-GITM.

Paul Withers, Collaborator has been involved in the investigation of the sources of variability in the Martian atmosphere and has recently been examining the effect of solar variability, such as solar flares, on the ionosphere [*Withers and Mendillo*, 2005; *Mendillo et al.*, 2006; *Withers et al.*, 2006; *Withers*, 2009]. Dr. Withers will provide assistance in interpretation of data sets that are relevant for investigating the atmospheric response to solar flares, and aid in interpretation of model results for solar flare simulations.

7.1 Schedule

Year 1 Within the first year, we will focus on analysis of the Martian upper atmospheric response to solar flares. We will use the Planetary Data System (PDS) to gather electron densities from the the MGS Radio Science experiment (during flare events), and corresponding neutral mass densities from the MGS and Odyssey acclerometers (when available). We will gather information about the EUV-XUV spectrum using FISM, and begin to classify each of the events discussed in Table 2 in terms of energy input and the response of the system that is observed in the data. Additionally, we will set up and conduct the M-GITM simulations for all of these events and investigate and quantify the differences between the modeled responses of the system to those observed. We will publish (JGR) our initial survey of the data analysis and modeling results on the upper atmospheric response to solar flares.

Year 2 During the second year, we will construct time dependent maps of the dust opacity for input into M-GITM and perform simulations of realistic dust storm events. We will quantify the response of the system to the dust storms and determine the reasons behind differences between the model results and the observations, and determine which characteristics of dust storm events lead to an upper atmospheric perturbation, and which have no effect on the upper atmosphere. We will publish the results (JGR) from our data analysis and modeling investigation into the effect of dust storms on the upper atmosphere.

Year 3 Finally, in year 3, we will rerun a subset of the solar flare and dust storm simulations over again, slightly altering the input conditions in order to determine how different the resulting upper atmospheric perturbations are due to the different input conditions. We will also setup idealized simulations that will address the "worst case" scenarios in which a solar flare event coincides with a dusty lower atmosphere and determine how different dust distributions affect the upper atmospheric response to solar flares. We will publish a paper (JGR) discussing the sensitivity of the system to ranges of input conditions as well as one addressing the affects of dust preconditioning.

References

Angelats i Coll, M., F. Forget, M. A. López-Valverde, P. L. Read, and S. R. Lewis, Upper atmosphere of Mars up to 120 km: Mars Global Surveyor accelerometer data analysis with the LMD general circulation model, *Journal of Geophysical Research (Planets)*, *109*, E01,011, doi:10.1029/2003JE002163, 2004.

Barabash, S., A. Fedorov, R. Lundin, and J.-A. Sauvaud, Martian Atmospheric Erosion Rates, *Science*, *315*, 501–, doi:10.1126/science.1134358, 2007.

Bougher, S., and D. Huestis, Solar cycle variation of Mars exospheric temperatures: Critical review of available dayside measurements and recent model simulations, in *38th COSPAR Scientific Assembly*, vol. 38, pp. 1410–+, 2010.

Bougher, S., G. Keating, R. Zurek, J. Murphy, R. Haberle, J. Hollingsworth, and R. T. Clancy, Mars global surveyor aerobraking : atmospheric trends and model interpretation, *Advances in Space Research*, *23*, 1887, doi:10.1016/S0273-1177(99)00272-0, 1999.

Bougher, S. W., and R. E. Dickinson, Mars mesosphere and thermosphere. I - Global mean heat budget and thermal structure, *J. Geophys. Res.*, *93*, 7325–7337, doi:10.1029/JA093iA07p07325, 1988.

Bougher, S. W., S. Engel, R. G. Roble, and B. Foster, Comparative terrestrial planet thermospheres 2. Solar cycle variation of global structure and winds at equinox, *J. Geophys. Res.*, *1041*, 16,591–16,611, doi:10.1029/1998JE001019, 1999.

Bougher, S. W., S. Engel, R. G. Roble, and B. Foster, Comparative terrestrial planet thermospheres 3. Solar cycle variation of global structure and winds at solstices, *J. Geophys. Res.*, *105*, 17,669–17,692, doi:10.1029/1999JE001232, 2000.

Bougher, S. W., S. Engel, D. P. Hinson, and J. M. Forbes, Mars Global Surveyor Radio Science electron density profiles: Neutral atmosphere implications, *Geophys. Res. Lett.*, *28*, 3091–3094, doi:10.1029/2001GL012884, 2001.

Bougher, S. W., S. Engel, D. P. Hinson, and J. R. Murphy, MGS Radio Science electron density profiles: Interannual variability and implications for the Martian neutral atmosphere, *Journal of Geophysical Research (Planets)*, *109*, E03,010, doi:10.1029/2003JE002154, 2004.

Bougher, S. W., J. M. Bell, J. R. Murphy, M. A. Lopez-Valverde, and P. G. Withers, Polar warming in the Mars thermosphere: Seasonal variations owing to changing insolation and dust distributions, *Geophys. Res. Lett.*, *330*, L02,203, doi:10.1029/2005GL024059, 2006.

Bougher, S. W., T. M. McDunn, K. A. Zoldak, and J. M. Forbes, Solar cycle variability of Mars dayside exospheric temperatures: Model evaluation of underlying thermal balances, *Geophys. Res. Lett.*, *360*, L05,201, doi:10.1029/2008GL036376, 2009.

Bougher, S. W., D. A. Brain, J. L. Fox, F. Gonzalez-Galindo, C. Simon-Wedlund, and P. G. Withers, *Chapter 14: Upper Atmosphere and Ionosphere*, Cambridge Unversity Press, 2011a.

Bougher, S. W., D. J. Pawlowski, and J. Murphy, Towards and Understanding of the Time Dependent Responses of the Martian Upper Atmosphere to Dust Events, in *Fall AGU, Session P04*, 2011b.

Bougher, S. W., A. Ridley, D. Pawlowski, J. M. Bell, and S. Nelli, Development and Validation of the Ground-To-Exosphere Mars GITM Code: Solar Cycle and Seasonal Variations of the Upper atmosphere, in *Mars Atmosphere: Modelling and observation*, edited by F. Forget & E. Millour, pp. 379–381, 2011c.

Bridger, A. F. C., and J. R. Murphy, Mars' surface pressure tides and their behavior during global dust storms, *J. Geophys. Res.*, *103*, 8587–8602, doi:10.1029/98JE00242, 1998.

Chamberlin, P. C., T. N. Woods, and F. G. Eparvier, Flare irradiance spectral model (fism): Daily component algorithms and results, *Space Weather*, *5*, S07,005, doi:10.1029/2007SW000316, 2007.

Chamberlin, P. C., T. N. Woods, and F. G. Eparvier, Flare irradiance spectral model (fism): Daily component algorithms and results, *Space Weather*, *6*, S05,001, doi:10.1029/2007SW000372, 2008.

Chassefière, E., and F. Leblanc, Mars atmospheric escape and evolution; interaction with the solar wind, *planss*, *52*, 1039–1058, doi:10.1016/j.pss.2004.07.002, 2004.

Deng, Y., and A. Ridley, Possible reasons for underestimating joule heating in global models: E-field variability, spatial resolution and vertical velocity, *J. Geophys. Res.*, doi: 10.1029/2006JA012006, 2007.

Deng, Y., A. Ridley, and W. Wang, Effect of the altitudinal variation of the gravitational acceleration on the thermosphere simulation, *Geophys. Res. Lett.*, *113*, A09,302, doi: 10.1029/2007JA013081, 2008.

Fox, J. L., Response of the Martian thermosphere/ionosphere to enhanced fluxes of solar soft X rays, *Journal of Geophysical Research (Space Physics)*, *109*, A11,310, doi:10.1029/ 2004JA010380, 2004.

Fox, J. L., and K. Y. Sung, Solar activity variations of the Venus thermosphere/ionosphere, *J. Geophys. Res.*, *106*, 21,305–21,336, doi:10.1029/2001JA000069, 2001.

Fox, J. L., and K. E. Yeager, MGS electron density profiles: Analysis of the peak magnitudes, *icarus*, *200*, 468–479, doi:10.1016/j.icarus.2008.12.002, 2009.

Fox, J. L., P. Zhou, and S. W. Bougher, The Martian thermosphere/ionosphere at high and low solar activities, *Advances in Space Research*, *17*, 203–218, doi:10.1016/ 0273-1177(95)00751-Y, 1996.

González-Galindo, F., F. Forget, M. A. López-Valverde, M. Angelats i Coll, and E. Millour, A ground-to-exosphere Martian general circulation model: 1. Seasonal, diurnal, and solar cycle variation of thermospheric temperatures, *Journal of Geophysical Research (Planets)*, *114*, E04,001, doi:10.1029/2008JE003246, 2009.

Haberle, R. M., J. L. Hollingsworth, A. Colaprete, A. F. C. Bridger, C. P. McKay, J. R. Murphy, J. Schaeffer, , and R. Freedman, The NASA/AMES Mars General Circulation Model: Model Improvements and comparison with observations, in *Published Conference Abstract, International Workshop: Mars Atmosphere Modelling and Observations*, 2003.

Hanson, W. B., S. Sanatani, and D. R. Zuccaro, The Martian ionosphere as observed by the Viking retarding potential analyzers, *J. Geophys. Res.*, *82*, 4351–4363, doi:10.1029/JS082i028p04351, 1977.

Hinson, D. P., R. A. Simpson, J. D. Twicken, G. L. Tyler, and F. M. Flasar, Initial results from radio occultation measurements with Mars Global Surveyor, *J. Geophys. Res.*, *1042*, 26,997–27,012, doi:10.1029/1999JE001069, 1999.

Hinteregger, H., K. Fukui, and B. Gibson, Observational, reference and model data on solar EUV from measurements on AE-E, *Geophys. Res. Lett.*, *8*, 1147, 1981.

Huestis, D. L., S. W. Bougher, J. L. Fox, M. Galand, R. E. Johnson, J. I. Moses, and J. C. Pickering, Cross Sections and Reaction Rates for Comparative Planetary Aeronomy, *Space Science Reviews*, *139*, 63–105, doi:10.1007/s11214-008-9383-7, 2008.

Keating, G. M., et al., The Structure of the Upper Atmosphere of Mars: In Situ Accelerometer Measurements from Mars Global Surveyor, *Science*, *279*, 1672–+, doi:10.1126/science.279.5357.1672, 1998.

Kim, J., A. F. Nagy, J. L. Fox, and T. E. Cravens, Solar cycle variability of hot oxygen atoms at Mars, *J. Geophys. Res.*, *1032*, 29,339–29,342, doi:10.1029/98JA02727, 1998.

López-Valverde, M. A., D. P. Edwards, M. López-Puertas, and C. Roldán, Non-local thermodynamic equilibrium in general circulation models of the Martian atmosphere 1. Effects of the local thermodynamic equilibrium approximation on thermal cooling and solar heating, *J. Geophys. Res.*, *1031*, 16,799–16,812, doi:10.1029/98JE01601, 1998.

Lundin, R., S. Barabash, A. Fedorov, M. Holmström, H. Nilsson, J.-A. Sauvaud, and M. Yamauchi, Solar forcing and planetary ion escape from Mars, *Geophys. Res. Lett.*, *350*, L09,203, doi:10.1029/2007GL032884, 2008.

Mahajan, K. K., N. K. Lodhi, and S. Singh, Ionospheric effects of solar flares at Mars, *Geophys. Res. Lett.*, *361*, L15,207, doi:10.1029/2009GL039454, 2009.

Martinis, C. R., J. K. Wilson, and M. J. Mendillo, Modeling day-to-day ionospheric variability on Mars, *Journal of Geophysical Research (Space Physics)*, *108*, 1383, doi:10.1029/2003JA009973, 2003.

McDunn, T. L., S. W. Bougher, J. Murphy, M. D. Smith, F. Forget, J.-L. Bertaux, and F. Montmessin, Simulating the density and thermal structure of the middle atmosphere (80-130 km) of Mars using the MGCM-MTGCM: A comparison with MEX/SPICAM observations, *icarus*, *206*, 5–17, doi:10.1016/j.icarus.2009.06.034, 2010.

Mendillo, M., S. Smith, J. Wroten, H. Rishbeth, and D. Hinson, Simultaneous ionospheric variability on Earth and Mars, *Journal of Geophysical Research (Space Physics)*, *108*, 1432, doi:10.1029/2003JA009961, 2003.

Mendillo, M., P. Withers, D. Hinson, H. Rishbeth, and B. Reinisch, Effects of Solar Flares on the Ionosphere of Mars, *Science*, *311*, 1135–1138, doi:10.1126/science.1122099, 2006.

MEPAG Goals Committee, N., Mars exploration program analysis group (mepag) science goals, 2010.

Moudden, Y., and J. M. Forbes, Topographic connections with density waves in Mars' aerobraking regime, *Journal of Geophysical Research (Planets)*, *113*, E11,009, doi:10.1029/2008JE003107, 2008.

Moudden, Y., and J. M. Forbes, A new interpretation of Mars aerobraking variability: Planetary wave-tide interactions, *Journal of Geophysical Research (Planets)*, *115*, E09,005, doi:10.1029/2009JE003542, 2010.

Murphy, J. R., O. B. Toon, R. M. Haberle, and J. B. Pollack, Numerical simulations of the decay of Martian global dust storms, *J. Geophys. Res.*, *951*, 14,629–14,648, doi:10.1029/JB095iB09p14629, 1990.

Murphy, J. R., J. B. Pollack, R. M. Haberle, C. B. Leovy, O. B. Toon, and J. Schaeffer, Three-dimensional numerical simulation of Martian global dust storms, *J. Geophys. Res.*, *1002*, 26,357–26,376, doi:10.1029/95JE02984, 1995.

Pawlowski, D., and A. Ridley, Modeling the thermospheric response to solar flares, *J. Geophys. Res.*, *113*, A10,309, doi:10.1029/2008JA013182, 2008.

Pawlowski, D., A. Ridley, I. Kim, and D. Bernstein, Global model comparison with millstone hill during September 2005, *J. Geophys. Res.*, *113*, A01,312, doi:10.1029/2007JA012390, 2008.

Pawlowski, D., S. Bougher, and A. Ridley, The effect of solar variability on the martian thermospher and ionosphere system, in *38th COSPAR Scientific Assembly*, vol. 38, pp. 1100–+, 2010.

Pawlowski, D. J., and A. J. Ridley, Modeling the ionospheric response to the 28 October 2003 solar flare due to coupling with the thermosphere, *Radio Science*, *44*, RS0A23, doi:10.1029/2008RS004081, 2009a.

Pawlowski, D. J., and A. J. Ridley, Quantifying the effect of thermospheric parameterization in a global model, *Journal of Atmospheric and Solar-Terrestrial Physics*, *71*, 2017–2026, doi:10.1016/j.jastp.2009.09.007, 2009b.

Pawlowski, D. J., and A. J. Ridley, The effects of different solar flare characteristics on the global thermosphere, *Journal of Atmospheric and Solar-Terrestrial Physics*, *73*(13), 1840 – 1848, doi:10.1016/j.jastp.2011.04.004, 2011.

Pawlowski, D. J., S. W. Bougher, and P. Chamberlin, Modeling the Response of the Martian Upper Atmosphere to Solar Flares, in *Fall AGU, Session SA06*, 2011.

Richards, P. G., J. A. Fennelly, and D. G. Torr, EUVAC: A solar EUV flux model for aeronomic calculations, *J. Geophys. Res.*, *99*, 8981, 1994.

Ridley, A., Y. Deng, and G. Tòth, The global ionosphere-thermosphere model, *J. Atmos. Sol-Terr. Phys.*, *68*, 839, 2006.

Roble, R. G., *Energetics of the Mesosphere and Thermosphere*, pp. 1–+, 1995.

Smith, D. E., and M. T. Zuber, The Shape of Mars and the Topographic Signature of the Hemispheric Dichotomy, in *Lunar and Planetary Institute Science Conference Abstracts*, *Lunar and Planetary Institute Science Conference Abstracts*, vol. 27, pp. 1221–+, 1996.

Smith, M. D., Interannual variability in TES atmospheric observations of Mars during 1999-2003, *icarus*, *167*, 148–165, doi:10.1016/j.icarus.2003.09.010, 2004.

Smith, M. D., THEMIS observations of Mars aerosol optical depth from 2002-2008, *icarus*, *202*, 444–452, doi:10.1016/j.icarus.2009.03.027, 2009.

Sutton, E., J. Forbes, R. Nerem, and T. Woods, Neutral density response to the solar flares of October and November, *Geophys. Res. Lett.*, *33*, L22,101, doi:10.1029/2006GL027737, 2003.

Tobiska, W., Revised solar extreme ultraviolet flux model, *J. Atm. Terr. Phys.*, *53*, 1005, 1991.

Torr, M., P. Richards, and D. Torr, A new determination of the ultraviolet heating efficiency, *J. Geophys. Res.*, *85*(A12), 6819, 1980.

Wang, J.-S., and E. Nielsen, Behavior of the Martian dayside electron density peak during global dust storms, *planss*, *51*, 329–338, doi:10.1016/S0032-0633(03)00015-1, 2003.

Withers, P., A review of observed variability in the dayside ionosphere of Mars, *Advances in Space Research*, *44*, 277–307, doi:10.1016/j.asr.2009.04.027, 2009.

Withers, P., and M. Mendillo, Response of peak electron densities in the martian ionosphere to day-to-day changes in solar flux due to solar rotation, *planss*, *53*, 1401–1418, doi:10.1016/j.pss.2005.07.010, 2005.

Withers, P., S. W. Bougher, and G. M. Keating, The effects of topographically-controlled thermal tides in the martian upper atmosphere as seen by the MGS accelerometer, *icarus*, *164*, 14–32, doi:10.1016/S0019-1035(03)00135-0, 2003.

Withers, P., M. Mendillo, J. Wroten, H. Rishbeth, D. Hinson, and B. Reinisch, Observations of the Effects of Solar Flares on Earth and Mars, *AGU Fall Meeting Abstracts*, pp. B1165+, 2005.

Withers, P., M. Mendillo, and D. Hinson, Space weather effects on the Mars ionosphere due to solar flares and meteors, in *European Planetary Science Congress 2006*, pp. 190–+, 2006.

Woods, T., and G. Rottman, Solar ultraviolet variability over time periods of aeronomic interest, *Atmospheres in the Solar System: Comparative Aeronomy, Geophys. Monogr. Ser.*, *130*, 221, 2002.

Woods, T. N., F. G. Eparvier, S. M. Bailey, P. C. Chamberlin, J. Lean, G. J. Rottman, S. C. Solomon, W. K. Tobiska, and D. L. Woodraska, Solar EUV Experiment (SEE): Mission overview and first results, *J. Geophys. Res.*, *110*, 1312–+, doi:10.1029/2004JA010765, 2005.